Dual-energy computed tomography in stroke imaging: technical and clinical considerations of virtual noncontrast images for detection of the hyperdense artery sign

Winklhofer, Sebastian ; De Martini, Ilaria Vittoria ; Nern, Chrisitian ; Blume, Iris ; Wegener, Susanne ; Pangalu, Athina ; Valavanis, Antonios ; Alkadhi, Hatem ; Guggenberger, Roman

Abstract: OBJECTIVE: The technical feasibility of virtual noncontrast (VNC) images from dual-energy computed tomography (DECT) for the detection of the hyperdense artery sign (HAS) in ischemic stroke patients was investigated. METHODS: True noncontrast (TNC) scans of 60 patients either with or without HAS (n = 30 each) were investigated. Clot presence and characteristics were assessed on VNC images from DECT angiography and compared with TNC images. Clot characterization included the level of confidence for diagnosing HAS, a qualitative clot burden score, and quantitative attenuation (Hounsfield unit [HU]) measurements. RESULTS: Sensitivity, specificity, and accuracy of VNC for diagnosing HAS were 97%, 90%, and 93%, respectively. No significant differences were found regarding the diagnostic confidence (P = 0.18) and clot burden score (P = 0.071). No significant HU differences were found among vessels with HAS in VNC (56 ± 7HU) and TNC (57 ± 8HU) (P = 0.691) images. CONCLUSIONS: Virtual noncontrast images derived from DECT enable an accurate detection and characterization of HAS.

DOI: https://doi.org/10.1097/RCT.0000000000000638

Dual-Energy Computed Tomography in Stroke Imaging: Technical and Clinical Considerations of Virtual Noncontrast Images for Detection of the Hyperdense Artery Sign

Sebastian Winklhofer, MD, Ilaria Vittoria De Martini, MD,* Chrisitian Nern, MD,* Iris Blume, MD,* Susanne Wegener, MD,† Athina Pangalu, MD,* Antonios Valavanis, MD,* Hatem Alkadhi, MD, MPH, EBCR,‡ and Roman Guggenberger, MD‡*

Objective: The technical feasibility of virtual noncontrast (VNC) images from dual-energy computed tomography (DECT) for the detection of the hyperdense artery sign (HAS) in ischemic stroke patients was investigated.

Methods: True noncontrast (TNC) scans of 60 patients either with or without HAS (n = 30 each) were investigated. Clot presence and characteristics were assessed on VNC images from DECT angiography and compared with TNC images. Clot characterization included the level of confidence for diagnosing HAS, a qualitative clot burden score, and quantitative attenuation (Hounsfield unit [HU]) measurements.

Results: Sensitivity, specificity, and accuracy of VNC for diagnosing HAS were 97%, 90%, and 93%, respectively. No significant differences were found regarding the diagnostic confidence ($P = 0.18$) and clot burden score ($P = 0.071$). No significant HU differences were found among vessels with HAS in VNC (56 ± 7HU) and TNC (57 ± 8HU) ($P = 0.691$) images.

Conclusions: Virtual noncontrast images derived from DECT enable an accurate detection and characterization of HAS.

Key Words: dual-energy computed tomography, hyperdense artery sign, ischemic stroke, thrombus

(*J Comput Assist Tomogr* 2017;00: 00–00)

The hyperdense artery sign (HAS) is caused by increased attenuation of acute thrombotic embolus in intracranial arteries on noncontrast computed tomography (CT).[1] It has a high specificity for the detection of complete vessel occlusion,[2,3] and presence of HAS is of prognostic importance because it is related to severe brain ischemia, a poor clinical outcome, and a higher mortality.[4–6] Furthermore, qualitative (eg, the clot burden) and quantitative clot characterizations (eg, Hounsfield units [HU]) on noncontrast CT are useful in predicting the effectiveness of intravenous (IV) recombinant tissue plasminogen activator therapy.[7,8] In addition, clot characterization is recently gaining in importance, because it is known as the main target in mechanical thrombectomy.[9]

Current concepts in acute stroke imaging suggest the acquisition of an initial noncontrast cranial CT in order to determine possible HAS and extent of thrombotic material and cerebral parenchymal damage. This is usually followed by contrast-enhanced scans including CT angiography (CTA) for the evaluation of the extracranial and intracranial vessels in order to determine the accurate thrombus localization and dynamic perfusion imaging for the evaluation of cerebral parenchymal integrity (tissue at risk).[1,10] In addition, postcontrast scans in venous phase are often appended in order to exclude pathologies such as tumor or venous thrombosis. Hence, radiation dose represents a major issue in acute stroke imaging both at onset and during follow-up.[11] In addition, contraindications to IV contrast application, that is, kidney failure, are frequent in stroke patients and require careful indications.

A promising application of dual-energy CT (DECT) is the generation of virtual noncontrast (VNC) images from postcontrast scans possibly obviating prior noncontrast imaging and optimizing diagnostic yield from IV contrast application.[12] By imaging at 2 tube potentials, the acquired high- and low-voltage data sets enable material decomposition because of the unique high- and low-kVp linear attenuation coefficients of a given material.[13,14] The postprocessing of postcontrast DECT images is based on the 3-material differentiation, which allows for a distinction of various materials such as iodine, blood, or calcifications.[13]

Recent studies have shown that VNC images generated from DECT may allow for replacing true noncontrast (TNC) images for the assessment of even subtle intracranial hemorrhage or after mechanical thrombectomy.[15,16] Further applications in the field of neuroradiology include the differentiation between tumor bleeding and pure hemorrhage, the differentiation between blood and iodine, or the automated bone removal in DECT angiography.[17–21]

Other than in CTA, where the proximal end of a thrombus is marked by the lack of luminal contrast with the rest of the thrombus being obscured, VNC images may also allow for thrombus characterization further distal including thrombus composition and length. At present, there is no study investigating the technical feasibility and diagnostic utility of VNC images from DECT for characterization of HAS in acute ischemic stroke. Hence, we hypothesized that VNC images could allow for accurate detection and characterization of acute arterial thrombotic emboli with an accuracy that is similar to that of standard TNC scans. Therefore, the aim of this study was to investigate the technical feasibility and the diagnostic utility of VNC images from DECT angiography for the detection of HAS in patients with acute thromboembolic ischemic stroke using TNC scans as standard of reference.

MATERIALS AND METHODS

Patient Selection

All procedures were performed in accordance with local and federal regulations and the Declaration of Helsinki. The

From the Departments of *Neuroradiology and †Neurology and ‡Institute of Diagnostic and Interventional Radiology, University Hospital Zurich, University of Zurich, Zurich, Switzerland.

Received for publication March 31, 2017; accepted April 24, 2017.

Correspondence to: Sebastian Winklhofer, MD, Department of Neuroradiology, University Hospital Zurich, Frauenklinikstrasse 10, 8091 Zurich, Switzerland (e-mail: sebastian.winklhofer@usz.ch).

The authors declare that all human and animal studies have been approved by the local ethics committee (KEK-ZH-Nr. 2014-0304) and have therefore been performed in accordance with the ethical standards laid down in the 1964 Declaration of Helsinki and its later amendments. The authors declare that all patients gave informed consent prior to inclusion in this study.

This research did not receive any specific grant from funding agencies in the public, commercial, or not-for-profit sectors.

The authors declare no conflict of interest.

DOI: 10.1097/RCT.0000000000000638

retrospective study was approved by the local ethics committee (2014–0304).

The patient group included 30 patients (16 women and 14 men; mean age, 68 years; age range, 36–90 years) with HAS in the middle cerebral artery (MCA) scanned between 2012 and 2014. Patients with HAS were identified through the institutional radiology information system with the search terms "hyperdense artery sign" and "hyperdense media sign" in the radiology reports. Inclusion criteria were the availability of TNC images and a DECT angiography of the same examination. Furthermore, the presence of a thrombus had to be confirmed by catheter angiography or magnetic resonance angiography within 12 hours.

Control Group

A total of 30 patients were included in the control group (closely age and sex matched; scanned with the same scanner in the same period; 12 women and 18 men; mean age, 53 years; age range, 21–87 years). Inclusion criteria were the availability of TNC images and a DECT angiography of the same examination. Exclusion criteria were suspected or known ischemia, presence of parenchymal hemorrhage, or presence of subarachnoidal hemorrhage. Furthermore, cases with pseudo-HAS as described elsewhere[22] were excluded. The CT indications for the control group were as follows: trauma (n = 11), tumor (n = 2), inflammation (n = 3), follow-up unruptured aneurysms (n = 5), headache (n = 5), other (n = 4).

CT Data Acquisition and Postprocessing

Cranial CT imaging was performed using a dual-source CT scanner (Somatom Definition; Siemens Healthcare, Erlangen, Germany) in single-energy mode for the TNC images and in dual-energy mode for CTA. Tube voltages were 120 kVp for single-energy mode, and 80 kVp and tin (Sn)–filtered 140 kVp in dual-energy mode.

Reference tube current–time product was set at 350 mAs/rotation for the TNC image acquisition and 222 and 111 mAs/rotation for the 80/Sn 140 kVp DECT angiography, respectively, using automated attenuation-based tube current modulation (CareDose 4D; Siemens). Slice collimation was 192 × 0.6 mm using the z-flying focal spot; gantry rotation time was 330 ms/rotation, and pitch was 0.8. Slice thickness was 0.75 mm; increment was 1.6 mm, using filtered back projection. For CTA acquisitions, an 80-mL bolus of iso-osmolar, nonionic iodinated contrast material (350 mg I/mL, Iobitridol [Xenetix 350; Guerbet, Aulnay-sous-Bois, France]) followed by a saline flush of 40 mL was injected into an antecubital vein with a dual-head power injector (Stellant; Medrad, Indianola, Pa) at a flow rate of 4.0 mL/s. Image initiation was controlled by bolus tracking with a region of interest (ROI) in the ascending aorta, using a 120-HU signal attenuation threshold. The image reconstruction was performed using a medium-smooth reconstruction kernel for DECT (D20f) and for SECT (H30s). The mean volume CT dose index of TNC images and that of DECT angiography were 61.8 ± 3.01 and 18.3 ± 2.96 mGy, respectively.

Postprocessing was performed by an independent radiologist who was not involved in the following image readout. All data sets were uploaded, postprocessed, and reconstructed on a dedicated workstation (syngo MultiModality Workplace, CT Dual-Energy, Virtual-Unenhanced application, syngo.via Client 3.0; Siemens Healthcare). The VNC images were calculated from DECT angiography data by using a 3-material decomposition algorithm.[13] Image reconstruction of TNC and VNC images was performed identically in axial, coronal, and sagittal planes. A slice thickness of 2.5 mm with an increment of 2.5 mm was selected for the optimal visualization of HAS[23] for both TNC and VNC images (Figs. 1 and 2).

Image Analysis

Image analysis of the TNC images was performed by 2 independent readers. Reader (R) 1 (R1, CN) is a board-certified neuroradiologist. R2 (SW) is a board-certified radiologist with experience as a neuroradiology fellow. The presence of HAS in the patient group and the absence of an HAS in the control group were confirmed by R1 and R2 in all cases. Disagreements between both readers were resolved by consensus. The TNC images were used as the reference standard. Both, R1 and R2 were not involved in the further readout regarding VNC images.

Image analysis of the VNC images was performed by 2 different, independent readers. R3 (IB) is a board-certified neuroradiologist with 8 years of experience. R4 (RG) is a board-certified radiologist with 2 years of experience as a neuroradiology fellow. Disagreements between readers were resolved by consensus.

All readers were blinded to the image acquisition parameters, clinical patient information, and to the results from the second reader. The readout was performed on high-resolution monitors (Flexscan MX 210; Eizo, Ishikawa, Japan), using the picture archiving and communication system (Agfa, Mortsel, Belgium) of the hospital. Image windowing was performed individually by each reader.

First, the presence and the extension of HAS in the TNC images were verified by R1 and R2 in a consensus readout. The

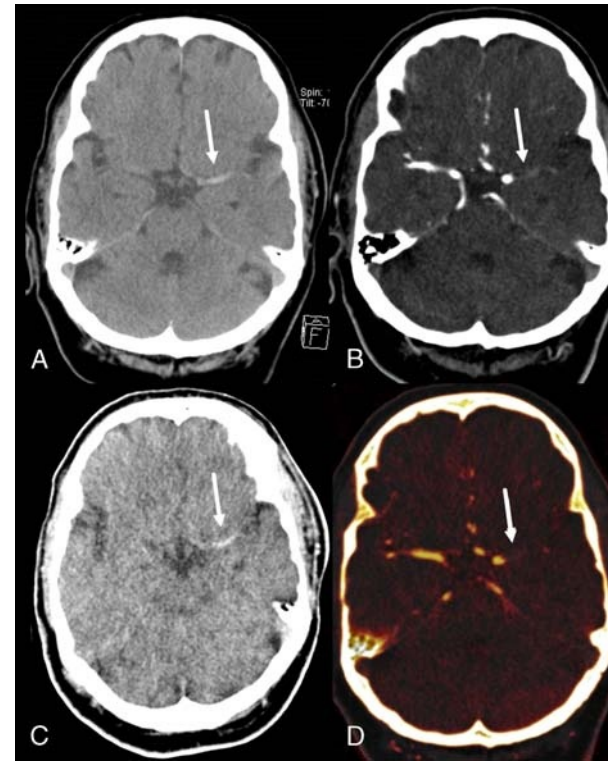

FIGURE 1. True noncontrast (A), CTA (B), VNC (C), and iodine (D) images of a 71-year-old male patient with acute ischemic stroke. C and D are postprocessed images from B. The HAS is clearly visible in both A and C (arrow). Note the vessel occlusion with the missing iodine contrast (arrow) in the CTA (B) and in the iodine (D) images compared with the contrast in the vessel on the contralateral side.

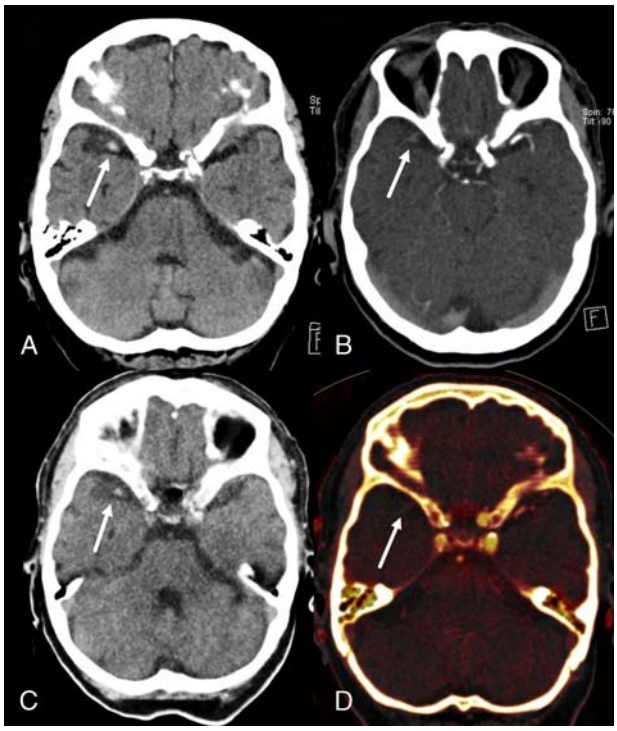

FIGURE 2. True noncontrast (A), CTA (B), VNC (C), and iodine (D) images of a 66-year-old female patient with acute ischemic stroke. The HAS is clearly visible in both the TNC and in the VNC images (C) (arrow). Note the vessel occlusion with the missing iodine contrast (arrow) in the CTA (B) and in the iodine (D) images compared with the contrast in the vessel on the contralateral side.

VNC images of all 60 cases (30 cases with HAS and 30 cases from the control group) were than presented in an arbitrary, randomized order to R3 and R4. To assess the intrareader agreement, R3 repeated the qualitative and quantitative readout after a time interval of 4 weeks to diminish recall bias.

Qualitative Readout

The qualitative readout included the evaluation of the presence or absence of an HAS in TNC and VNC images according to the following previously published criteria[24]: (1) spontaneous visibility of the whole horizontal part of the MCA, (2) attenuation of the MCA higher than that of the surrounding brain, (3) disappearance on bone windows, (4) unilaterality, and (5) absence of subarachnoid hemorrhage. Furthermore, the level of confidence for the presence of HAS was assessed using an adapted 4-point Likert scale[25]: 0 = definitively no HAS present, 1 = HAS probably not present, 2 = HAS probably present, and 3 = HAS definitively present. Score of 2 or 3 was defined as positive HAS sign. In order to determine the extent of thrombus, the clot burden score (CBS) was calculated for all VNC and TNC cases with HAS. Previous studies have shown the value of the CBS for the prediction of outcome after acute ischemic stroke.[26–28] The CBS is based on a 10- to 0-point score, with a score of 10 points implying clot absence and 0 points implying a complete multisegmental vessel occlusion.[26,27] In brief, 2 points are subtracted from the initial 10 points if thrombus is detected in one of the supraclinoid internal carotid arteries (ICAs), the proximal half of the MCA trunk, or/and the distal half of MCA trunk; 1 point is subtracted if thrombus is found in the infraclinoid ICA and for each affected M2 branch.[26] Care was taken to avoid misinterpretation of pseudo-HAS conditions, such as calcified atherosclerotic plaques.[22]

Quantitative Readout

In all cases with an HAS in TNC images, quantitative measurements of the vessel attenuation (HU) were performed in TNC and VNC images. Therefore, ROI measurements of the attenuation and SDs of the hyperdense MCA were performed with the standard metric software. An elliptical ROI was placed within axial slices in the area of the highest density of the vessel, taking care to avoid areas of inhomogeneity (ie, vessel borders, surrounding soft tissue). In cases of HAS in MCA vessels, the same procedure was repeated on the corresponding nonaffected artery on the contralateral side.[29]

Statistical Analysis

Continuous variables were defined as mean ± SD or median and range. Categorical variables were defined as frequencies and percentages. The Shapiro-Wilk test was conducted to test for normality of quantitative data.

Cohen κ coefficients were calculated to evaluate the interreader and intrareader agreement regarding the assessment of presence or absence of HAS in VNC images; κ values between 0.41 and 0.75 were interpreted as fair to good, and values between 0.75 and 1 were interpreted as excellent according to criteria originally proposed by Landis and Koch.[30,31]

Interreader and intrareader agreements regarding CT number measurements of HAS and the contralateral, unaffected vessel were analyzed using intraclass correlation coefficients. Intraclass correlation coefficients between 0.81 and 1.00 were interpreted as excellent.[30]

Sensitivity, specificity, and accuracy for the correct assessment of the presence or absence of HAS in VNC were calculated. Confidence intervals (CIs) were computed at a level of 95%. The TNC images were used as reference standard.

The Wilcoxon signed ranks test was conducted to compare the CBS among TNC and VNC images.

$P < 0.05$ was considered statistically significant. Statistical analyses were conducted using commercially available software (IBM SPSS Statistics, version 21.0; IBM Corp, Armonk, NY).

RESULTS

Interreader and Intrareader Agreement

The interreader and intrareader agreement regarding the presence of HAS in VNC images was excellent (κ = 0.76 and 0.82, respectively; both $P < 0.0001$). The ROI measurements demonstrated an excellent agreement regarding HU for interreader and intrareader analysis (intraclass correlation coefficient = 0.94 and 0.97, respectively; both $P < 0.0001$). Hence, the mean of both measurements was taken for further analysis.

Qualitative Results

The sensitivity, specificity, and accuracy of VNC images for the diagnosis of presence of HAS were as follows: 96.7% (95% CI, 0.828–0.999), 90.0% (95% CI, 0.735–0.979), and 93.3%, respectively.

No significant differences were found regarding the clot burden and extension with a median CBS in both TNC and VNC images of 7 ($P = 0.071$).

The median value for the level of confidence was 3 in TNC and in VNC images, without any significant difference ($P = 0.18$).

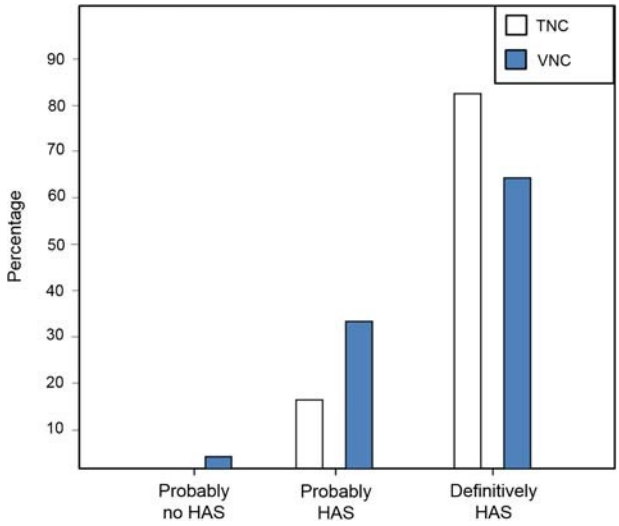

FIGURE 3. Level of confidence for the diagnosis of HAS in TNC and VNC CT images derived from DECT.

Details about the level of confidence in cases with HAS are shown in Figure 3. The level of confidence in VNC images of the control group was 0 (definitively no HAS): 22 cases (73%), 1 (probably no HAS): 5 cases (17%), 2 (probably HAS): 3 cases (10%), and 3 (definitely HAS): 0 cases.

Quantitative Results

Mean HUs were significantly different among vessels with HAS (56 ± 7 HU) and the contralateral, unaffected MCA (33 ± 8 HU) in VNC images ($P < 0.05$).

No significant differences were found between vessels with HAS in VNC (mean, 56 ± 7HU) and the corresponding HU measurement of the same vessel in the TNC images (mean, 57 ± 8HU) ($P = 0.691$). Similarly, no significant differences were found between vessels without HAS in VNC (mean, 33 ± 8HU) and the corresponding HU measurement of the same vessel in the TNC images (mean, 35 ± 5HU) ($P = 0.059$) (Fig 4).

Potential Radiation Dose Saving

The mean total volume CT dose index of VNC (18.3 ± 2.96 mGy) and TNC (61.8 ± 3.01 mGy) images was 80.1 mGy in TNC images. In cases of discarding the TNC images, this would have resulted in a potential mean radiation dose saving of 77% of the total radiation dose.

DISCUSSION

This study demonstrates the feasibility of using VNC images derived from DECT angiography images for the diagnosis of HAS in acute ischemic stroke patients. In addition, the high sensitivity, specificity, and accuracy for the presence of HAS in VNC images suggest that this technique is almost equally robust as TNC imaging and could be used to rule out HAS as an early sign of ischemic stroke and vessel occlusion with comparable diagnostic performance, respectively. Furthermore, the subjective level of confidence of the reading radiologists for the diagnosis of HAS in VNC images was comparable to the diagnosis of HAS in TNC images.

In addition to demonstrating the technical feasibility and potential diagnostic utility for HAS in VNC images postprocessed from DECT angiography, we were also interested if there were any differences between prognostic appraisals based on qualitative clot characterization.[8] We found slight but nonsignificant differences in the CBS among VNC and the corresponding TNC images. We believe that they are caused by decreased sensitivity for distal small vessel occlusions in VNC compared with TNC images due to lower tube potential and consecutive higher background image noise in DECT angiography. All emboli of the main trunk (ICA, M1), however, were visible in VNC images in all cases.

Our study showed highly consistent attenuation values between VNC and TNC images, suggesting that the applied DECT decomposition algorithm is robust and allows for calculation of highly reliable noncontrast attenuation profiles. Quantitative attenuation values in HU of vessels with HAS in VNC images are in a comparable range with results from previous studies investigating HU measurements in TNC images.[7,32] Hence, absolute HU from VNC images in HAS could be used for clinical prognostic appraisals as suggested by previous studies.[7,33]

Jiang et al[15] stated that the image quality of VNC images generated from DECT angiography is characterized by a higher image noise level and markedly reduced contrast between gray and white matter compared with TNC images. This might result in a compromised discrimination of subtle signs of infarct demarcation. Even though image quality was not a focus of the present study, it might be interesting to investigate this in future DECT applications. The VNC images are generated from DECT angiography images, acquired with essentially different imaging parameters compared with TNC images. One of the main differences is the commonly lower tube current in DECT angiography.[11] However, the tube current can be manually influenced with higher mAs until the contrast-to-noise ratio is at a level allowing for a confident assessment of cortical gray and white matter.[34] Additional studies are warranted to assess whether VNC images allow for the detection of other relevant imaging findings in stroke patients such as the insular ribbon sign or demarcated infarctions. However, this was beyond the focus of our study. Nevertheless, modern CT imaging concepts aim for a reduction of radiation dose without losing essential image information. If VNC images will turn out to be equally robust and potentially able to replace TNC acquisitions, this would result in a considerable radiation dose reduction as already suggested by Jiang et al.[15] Our study supports this notion because discarding the TNC image acquisition would have resulted in a mean radiation dose reduction of

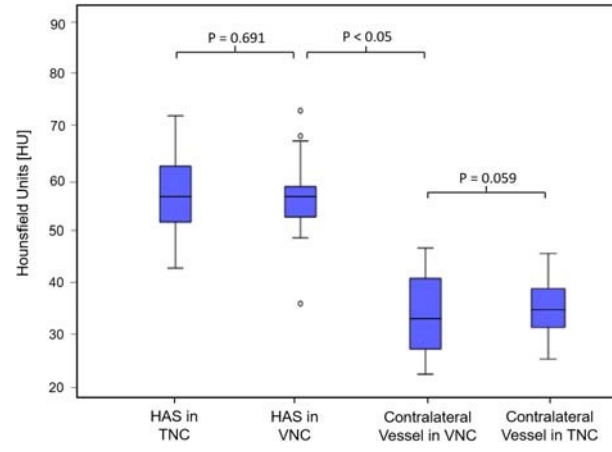

FIGURE 4. Quantitative results from CT attenuation measurements of HAS and the contralateral, unaffected vessel on TNC images versus VNC images.

more than 61 mGy. Furthermore, most relevant findings from TNC images, for example, extent of infarct demarcation or possible underlying neoplastic conditions, can also be detected in commonly acquired late-phase (venous phase) head CT, which is commonly performed after TNC and CTA image acquisitions using approximately the same radiation dose as TNC scans.

Even though a very high sensitivity of 97% was demonstrated for the detection of HAS, one of the cases was missed in VNC images. In retrospect, having the TNC and the VNC images next to each other, HAS was indeed slightly visible in this particular case, and we believe that this was missed because of its peripheral location (M2 segment) and a relatively high image noise in the surrounding brain tissue. The latter might compromise detection of peripheral HAS and lead to slightly lower confidence score in VNC images as shown in this study. On the other hand, calculated iodine maps can be overlaid on VNC images. Thereby, the exact localization of embolic vessel obstruction can be depicted more confidently by a lack of contrast material in the vessel lumen distal to the obstruction site. The described technique might furthermore be helpful in cases of previous contrast agent application with remnants of contrast agent in the vessel system, which might mask HAS and thus lead to higher confidence for the reading physician.

Study Limitations

First, we did not assess image noise and depiction quality of brain parenchyma on VNC images. Both potentially impact the comprehensive assessment of brain damage and will be the focus of further studies on DECT in stroke imaging. Second, we did not investigate the influence of the hematocrit on the quantitative and qualitative image analysis. However, because we were using the TNC images as reference standard, we believe that the corresponding DECT angiography images should have been affected in a similar way. Finally, in cases of large and obvious ischemic demarcations, blinding was not fully possible.

CONCLUSIONS

The VNC images derived from DECT enable an accurate detection and characterization of HAS compared with standard TNC scans.

REFERENCES

1. Bouchez L, Sztajzel R, Vargas MI, et al. CT imaging selection in acute stroke [published online ahead of print October 26, 2016]. *Eur J Radiol*. 2016.
2. Ernst M, Romero JM, Buhk JH, et al. Sensitivity of visual and quantitative detection of middle cerebral artery occlusion on non–contrast-enhanced computed tomography. *Neuroradiology*. 2014;56:1063–1068.
3. Mair G, Boyd EV, Chappell FM, et al. Sensitivity and specificity of the hyperdense artery sign for arterial obstruction in acute ischemic stroke. *Stroke*. 2015;46:102–107.
4. Kharitonova T, Ahmed N, Thoren M, et al. Hyperdense middle cerebral artery sign on admission CT scan—prognostic significance for ischaemic stroke patients treated with intravenous thrombolysis in the safe implementation of thrombolysis in Stroke International Stroke Thrombolysis Register. *Cerebrovasc Dis*. 2009;27:51–59.
5. Novotna J, Kadlecova P, Czlonkowska A, et al. Hyperdense cerebral artery computed tomography sign is associated with stroke severity rather than stroke subtype. *J Stroke Cerebrovasc Dis*. 2014;23:2533–2539.
6. Lam WW, Leung TW, Chu WC, et al. Hyperacute extensive middle cerebral artery territory infarcts. Role of computed tomography in predicting outcome. *J Comput Assist Tomogr*. 2004;28:650–653.
7. Puig J, Pedraza S, Demchuk A, et al. Quantification of thrombus Hounsfield units on noncontrast CT predicts stroke subtype and early recanalization after intravenous recombinant tissue plasminogen activator. *AJNR Am J Neuroradiol*. 2012;33:90–96.
8. Mair G, von Kummer R, Morris Z, et al. Effect of alteplase on the CT hyperdense artery sign and outcome after ischemic stroke. *Neurology*. 2016;86:118–125.
9. Goyal M, Demchuk AM, Menon BK, et al. Randomized assessment of rapid endovascular treatment of ischemic stroke. *N Engl J Med*. 2015;372:1019–1030.
10. Verro P, Tanenbaum LN, Borden NM, et al. CT angiography in acute ischemic stroke: preliminary results. *Stroke*. 2002;33:276–278.
11. Diekmann S, Siebert E, Juran R, et al. Dose exposure of patients undergoing comprehensive stroke imaging by multidetector-row CT: comparison of 320-detector row and 64-detector row CT scanners. *AJNR Am J Neuroradiol*. 2010;31:1003–1009.
12. De Cecco CN, Boll DT, Bolus DN, et al. White paper of the Society of Computed Body Tomography and Magnetic Resonance on dual-energy CT, part 4: abdominal and pelvic applications. *J Comput Assist Tomogr*. 2017;41:8–14.
13. Johnson TR, Krauss B, Sedlmair M, et al. Material differentiation by dual energy CT: initial experience. *Eur Radiol*. 2007;17:1510–1517.
14. Siegel MJ, Kaza RK, Bolus DN, et al. White paper of the Society of Computed Body Tomography and Magnetic Resonance on dual-energy CT, part 1: technology and terminology. *J Comput Assist Tomogr*. 2016;40:841–845.
15. Jiang XY, Zhang SH, Xie QZ, et al. Evaluation of virtual noncontrast images obtained from dual-energy CTA for diagnosing subarachnoid hemorrhage. *AJNR Am J Neuroradiol*. 2015;36:855–860.
16. Gariani J, Cuvinciuc V, Courvoisier D, et al. Diagnosis of acute ischemia using dual energy CT after mechanical thrombectomy. *J Neurointerv Surg*. 2016;8:996–1000.
17. Phan CM, Yoo AJ, Hirsch JA, et al. Differentiation of hemorrhage from iodinated contrast in different intracranial compartments using dual-energy head CT. *AJNR Am J Neuroradiol*. 2012;33:1088–1094.
18. Kim SJ, Lim HK, Lee HY, et al. Dual-energy CT in the evaluation of intracerebral hemorrhage of unknown origin: differentiation between tumor bleeding and pure hemorrhage. *AJNR Am J Neuroradiol*. 2012;33:865–872.
19. Morhard D, Fink C, Graser A, et al. Cervical and cranial computed tomographic angiography with automated bone removal: dual energy computed tomography versus standard computed tomography. *Invest Radiol*. 2009;44:293–297.
20. Brockmann C, Scharf J, Nolte IS, et al. Dual-energy CT after peri-interventional subarachnoid haemorrhage: a feasibility study. *Clin Neuroradiol*. 2010;20:231–235.
21. Zhang LJ, Wu SY, Poon CS, et al. Automatic bone removal dual-energy CT angiography for the evaluation of intracranial aneurysms. *J Comput Assist Tomogr*. 2010;34:816–824.
22. Jha B, Kothari M. Pearls & oy-sters: hyperdense or pseudohyperdense MCA sign: a Damocles sword? *Neurology*. 2009;72:e116–e117.
23. Riedel CH, Jensen U, Rohr A, et al. Assessment of thrombus in acute middle cerebral artery occlusion using thin-slice nonenhanced computed tomography reconstructions. *Stroke*. 2010;41:1659–1664.
24. Leys D, Pruvo JP, Godefroy O, et al. Prevalence and significance of hyperdense middle cerebral artery in acute stroke. *Stroke*. 1992;23:317–324.
25. Connell L, Koerte IK, Laubender RP, et al. Hyperdense basilar artery sign-a reliable sign of basilar artery occlusion. *Neuroradiology*. 2012;54:321–327.
26. Tan IY, Demchuk AM, Hopyan J, et al. CT angiography clot burden score and collateral score: correlation with clinical and radiologic outcomes in

acute middle cerebral artery infarct. *AJNR Am J Neuroradiol*. 2009;30: 525–531.

27. Puetz V, Dzialowski I, Hill MD, et al. Intracranial thrombus extent predicts clinical outcome, final infarct size and hemorrhagic transformation in ischemic stroke: the clot burden score. *Int J Stroke*. 2008;3: 230–236.
28. Topcuoglu MA, Arsava EM, Akpinar E. Clot characteristics on computed tomography and response to thrombolysis in acute middle cerebral artery stroke. *J Stroke Cerebrovasc Dis*. 2015;24:1363–1372.
29. Haridy J, Churilov L, Mitchell P, et al. Is there association between hyperdense middle cerebral artery sign on CT scan and time from stroke onset within the first 24-hours? *BMC Neurol*. 2015;15:101.
30. Landis JR, Koch GG. The measurement of observer agreement for categorical data. *Biometrics*. 1977;33:159–174.
31. Kirkwood BR, Sterne JAC, Kirkwood BR. *Essential Medical Statistics*. 2nd ed. Malden, MA: Blackwell Science; 2003.
32. Koo CK, Teasdale E, Muir KW. What constitutes a true hyperdense middle cerebral artery sign? *Cerebrovasc Dis*. 2000;10:419–423.
33. Shobha N, Bal S, Boyko M, et al. Measurement of length of hyperdense MCA sign in acute ischemic stroke predicts disappearance after IV tPA. *J Neuroimaging*. 2014;24:7–10.
34. Becker HC, Augart D, Karpitschka M, et al. Radiation exposure and image quality of normal computed tomography brain images acquired with automated and organ-based tube current modulation multiband filtering and iterative reconstruction. *Invest Radiol*. 2012;47:202–207.